

Strut-and-tie model of deep beams with web openings - An optimization approach

Hong Guan[†]

*School of Engineering, Griffith University Gold Coast Campus, PMB 50 Gold Coast Mail Centre,
Queensland 9726, Australia*

(Received June 28, 2003, Accepted November 10, 2004)

Abstract. Reinforced concrete deep beams have useful applications in tall buildings and foundations. Over the past two decades, numerous design models for deep beams were suggested. However even the latest design manuals still offer little insight into the design of deep beams in particular when complexities exist in the beams like web openings. A method commonly suggested for the design of deep beams with openings is the strut-and-tie model which is primarily used to represent the actual load transfer mechanism in a structural concrete member under ultimate load. In the present study, the development of the strut-and-tie model is transformed to the topology optimization problem of continuum structures. During the optimization process, both the stress and displacement constraints are satisfied and the performance of progressive topologies is evaluated. The influences on the strut-and-tie model in relation to different size, location and number of openings, as well as different loading and support conditions in deep beams are examined in some detail. In all, eleven deep beams with web openings are optimized and compared in nine groups. The optimal strut-and-tie models achieved are also compared with published experimental crack patterns. Numerical results have shown to confirm the experimental observations and to efficiently represent the load transfer mechanism in concrete deep beams with openings under ultimate load.

Key words: concrete deep beams; strut-and-tie model; web openings; support conditions; topology optimization; stress and displacement constraints.

1. Introduction

A reinforced concrete deep beam is a type of non-flexural member, which is generally defined as a member that has a span to depth ratio of less than 5. Deep beams have useful applications in tall buildings and foundations. More specifically deep beams are used in the following applications including transfer girders, pile caps, foundation walls and offshore structures. Over the past two decades, as the need for deep beams continued to grow throughout the construction industry, numerous design models for deep beams were suggested. However even the latest design manuals, such as the ACI code (2002), Eurocode (1992), the British (1997) and Australian Standards (2002) still offer little insight into the design of deep beams in particular when complexities exist in the beams like web openings.

[†] Senior Lecturer, E-mail: H.Guan@griffith.edu.au

In various forms of construction, openings in the web area of deep beams are frequently provided for accessibility and to allow essential services to pass through the beam. The presence of openings induces geometric discontinuity into the deep beams, which only enhances the complexity of the nonlinear stress distribution over the depth of the beams. Numerous investigations have been conducted into various attributes of deep beams (Rogowsky *et al.* 1986, Kong 1990, Tan *et al.* 1995, 1997a, b & c, Ashour 1997, Foster and Gilbert 1998, Tan *et al.* 2003a). However only limited research has been conducted dealing with deep beams with web openings (Mansur and Alwis 1984, Almeida and Pinto 1999, Maxwell and Breen 2000, Ashour and Rishi 2000, Tan *et al.* 2003b).

A method commonly suggested for the design of deep beams with openings is the strut-and-tie model which is primarily used to represent the actual load transfer mechanism in a structural concrete member under ultimate load. However many of the ways used in deriving the strut-and-tie model can be laborious and complex, because the compression strut from the loaded area generally separates and tracks around the opening before joining together again at the supports. This is especially true when predicting the correct strut-and-tie model for members with complex loading, support and geometric conditions (various location and size of openings) (Parsons and Guan 2003). Hence it would be advantageous if a simple and effective method of generating the strut-and-tie model can be derived.

In the engineering research field, fast, accurate and reliable methods of design are increasingly sort after. As new technology and ideas are generated, better design methods maybe established. In recent years structural optimization has become an area emerging that has the possibility of modifying classical design. In this study, the development of the strut-and-tie model is transformed to the topology optimization problem of continuum structures. The optimal strut-and-tie model is generated by gradually removing inefficient material from an over-designed area. During the optimization process, both the stress and displacement constraints are satisfied and the performance of progressive topologies is evaluated.

In the present study, the influences on the strut-and-tie model in relation to (a) different size, location and number of openings; (b) different loading conditions; and (c) different support conditions are examined, through a detailed investigation on eleven deep beams with web openings. All the eleven beams are optimized and compared in nine groups. The optimal strut-and-tie models achieved are also compared with published experimental crack patterns.

2. Topology optimization of continuum structures

2.1 General

In the present study, the development of the strut-and-tie model of deep beams with openings is transformed to a topology optimization problem of continuum structures. In the design of a reinforced concrete member, the unknown location and the amount of reinforcement are to be determined. The designer needs to establish the strut-and-tie layout in a structural concrete member in order to reinforce it. As a result, the nonlinear behaviour of reinforced concrete is not considered in this study. A plain concrete member with assumed homogeneous continuum behaviour is thus analyzed. A linear elastic behaviour of cracked concrete is also assumed, and the progressive cracking of concrete is characterised by gradually eliminating concrete from the structural member,

eventually leading to a fully cracked stage at the optimum (Liang *et al.* 2000).

The objective of this topology optimization is to maximise the performance of an initial continuum design domain in terms of material efficiency and overall stiffness. This is achieved by gradually eliminating, from a discretised concrete member, a small number of elements with lowest von Mises stress and lowest displacement sensitivity number.

2.2 Optimization with stress and displacement constraints

To commence an optimization process of a deep beam, a finite element analysis is performed first, based on which the von Mises stress of each element σ_{vM}^e and the maximum von Mises stress of the structure $\sigma_{vM, \max}$ are evaluated. A deletion criterion can be obtained using the rejection ratio RR_i in conjunction with $\sigma_{vM, \max}$. This deletion criterion is the stress at which all elements with a lower stress are deemed insignificant. As such, an element is identified as lowly stressed if its σ_{vM}^e is less than the deletion criterion (Xie and Steven 1997) or

$$\sigma_{vM}^e \leq RR_i \times \sigma_{vM, \max} \quad (1)$$

A small value of RR_i (0.1%) is used in the present study to ensure that only a small number of lowly stressed elements N_s are identified each time, where i indicates the iteration number.

In addition to the stress constraint, the displacement of a structure has to be controlled. This is to ensure that whilst the lowly stressed (redundant) material is removed from the structure, the remaining part of the structure is still stiff enough and its maximum deflection will not exceed the prescribed limit. When the specified displacement limit is reached, the optimization procedure will be terminated. The displacement control is performed by evaluating a displacement sensitivity number based on the formulas proposed by Xie and Steven (1997).

In a finite element analysis, the static behaviour of a structure can be expressed by the stiffness equation as

$$\mathbf{K} \cdot \mathbf{u} = \mathbf{P} \quad (2)$$

where \mathbf{K} is the global stiffness matrix of a structure and, \mathbf{u} and \mathbf{P} are, respectively, the global nodal displacement and nodal load vectors. Assuming that the element i ($i = 1, N$) is to be removed from a structure where N is the total number of elements in the design domain. This would lead to a change in the stiffness matrix, $\Delta\mathbf{K}_i$, as well as a change in the displacement vector $\Delta\mathbf{u}$. However, it is assumed that the element removal has little effect on the load vector. By manipulating the modified stiffness equation, the change in the specified j th displacement component u_j due to the removal of the i th element can be represented by the displacement sensitivity number $\alpha_{d,i}$. Or,

$$\alpha_{d,i} = |\alpha_{d,ij}| = \left| \mathbf{u}_{ij}^T \cdot \mathbf{K}_i \cdot \mathbf{u}_i \right| \quad (3)$$

where $\alpha_{d,ij}$ can be positive or negative. Note in the design process that the j th displacement component u_j is to be limited to a prescribed value, u_j^* (i.e., $|u_j| \leq u_j^*$). Also in Eq. (3), \mathbf{u}_i and \mathbf{u}_{ij} are respectively the displacement vectors of the i th element due to the real load \mathbf{P} and due to the virtual unit load \mathbf{F}_j ; \mathbf{K}_i is the stiffness matrix of the i th element and is equal but opposite to $\Delta\mathbf{K}_i$. In more general cases when a structure is subjected to multiple load cases \mathbf{P}_k ($k = 1, L$) with multiple

prescribed displacement values u_{jk}^* ($j = 1, M$), the sensitivity number can then be derived as

$$\alpha_{d,i} = \sum_{k=1}^L \sum_{j=1}^M \lambda_{jk} \cdot |\alpha_{d,ijk}| = \sum_{k=1}^L \sum_{j=1}^M \lambda_{jk} \cdot |\mathbf{u}_{ij}^T \cdot \mathbf{K}_i \cdot \mathbf{u}_{ik}| \quad (i = 1, N) \quad (4)$$

in which \mathbf{u}_{ik} is the displacement vector of the i th element due to load case \mathbf{P}_k ; L and M are respectively the total number of load cases and that of displacement constraints. In Eq. (4), $\lambda_{jk} = |u_{jk}|/u_{jk}^*$ is the weighting parameter indicating the contribution of the j th displacement constraint under the k th load case.

In the optimization process, the sensitivity number $\alpha_{d,i}$ is evaluated for a total number of N_s elements that satisfy the stress condition as given in Eq. (1) (Guan *et al.* 2001). To minimize the change in displacement, a number of elements N_d with the lowest $\alpha_{d,i}$ are removed. In the present study, $N_d = 10$ has been found to produce satisfactory results.

The finite element analysis followed by systematic removal of lowly stressed elements forms an optimization cycle where RR_i remains constant. Such cycle or iteration is continued until no more elements are removed. To proceed to the next iteration, RR_i is increased by adding an evolution ratio ER , which is also taken as 0.1%. The repeated cycle of optimization process continues until a desired topology is obtained.

2.3 Determination of optimal strut-and-tie model

As the optimization cycle progresses, the resulting topology improves with increase in iteration. To identify the final topology which can be translated to the optimal strut-and-tie model, a performance index PI_d , which is used as the objective function, can be derived based on the scaling design concept (Liang *et al.* 2000) where the actual design variable such as the element thickness is scaled with respect to the design constraint. The topology optimization of a continuum structure can be posed in the following form:

$$\text{minimize} \quad V = \sum_{e=1}^N V_e \quad (5)$$

$$\text{subject to} \quad |u_{jk}| \leq u_{jk}^* \quad (j = 1, M; k = 1, L) \quad (6)$$

where V and V_e are respectively the volume of the total design domain and that of the element e . Note in the present study that minimizing the volume is equivalent to minimizing the weight, because a single type of material, i.e., plain concrete, is assumed for the entire design domain. For linear elastic plane stress problems, the structural stiffness matrix is a linear function of the design variable such as the thickness or the volume of the structure. To produce the most efficient topology with minimum weight, the volume of the design domain can be scaled with respect to the displacement constraint, with the aim of the j th displacement component under the k th load case (u_{jk}) reaching the prescribed displacement value u_{jk}^* . As a result, the relative volume of the initial (original) design domain, V'_o , can be expressed as

$$V'_o = V_o \cdot (|u_{jk}|_o / u_{jk}^*) \quad (7)$$

in which V_o and $|u_{jk}|_o$ are respectively the volume of, and the $|u_{jk}|$, in the original design domain. In an iterative optimization process, the relative volume of the current design (at the i th iteration), V'_i , can also be scaled as

$$V'_i = V_i \cdot (|u_{jk}|_i / u_{jk}^*) \quad (8)$$

where V_i and $|u_{jk}|_i$ are respectively the volume of, and the $|u_{jk}|$, in the current design domain (at the i th iteration).

The performance index PI_d at the i th iteration can then be determined as

$$PI_d = \frac{V'_o}{V'_i} = \frac{|u_{jk}|_o \cdot V_o}{|u_{jk}|_i \cdot V_i} \quad (9)$$

During the optimization process, PI_d measures the efficiencies of the progressive topologies. As the optimization procedure continues, the number of iterations increases while PI_d is maximized, until a certain point where the efficiency or performance of the topology declines. The maximum value of PI_d corresponds to the most efficient topology, which would lead to the optimal strut-and-tie model.

2.4 Optimization procedure

The proposed optimization procedure considering both stress and displacement constraints is presented in Fig. 1.

3. Deep beam models

In the present study, five factors viz the number, size and location of openings, as well as the loading and support conditions in deep beams are examined. This is done through the optimization of eleven beam models, designated as DB1 to DB11. An illustrative diagram of a deep beam is given in Fig. 2 where the size and location of the web openings are indicated symbolically. Details and configurations of the beam models are presented in Table 1 and Fig. 3, respectively.

All the deep beam models are optimized under both stress and displacement constraints. For the symmetrical beams under symmetrical loading, only half of the model is analyzed. The displacement limit is imposed under the point load. The numerical results compared in nine groups are presented in the following three sections. Included in the comparison are the configurations of the beams, the initial, intermediate and final topologies, the optimal strut-and-tie models, as well as available experimental crack patterns. Note that the final topology is determined when the performance index PI_d reaches the maximum value. Note also that in the strut-and-tie models, the solid lines represent the tension ties while the dash lines denote the compression struts. As a typical example, the PI_d curve and the volume reduction curve are also presented for beams in Group 8.

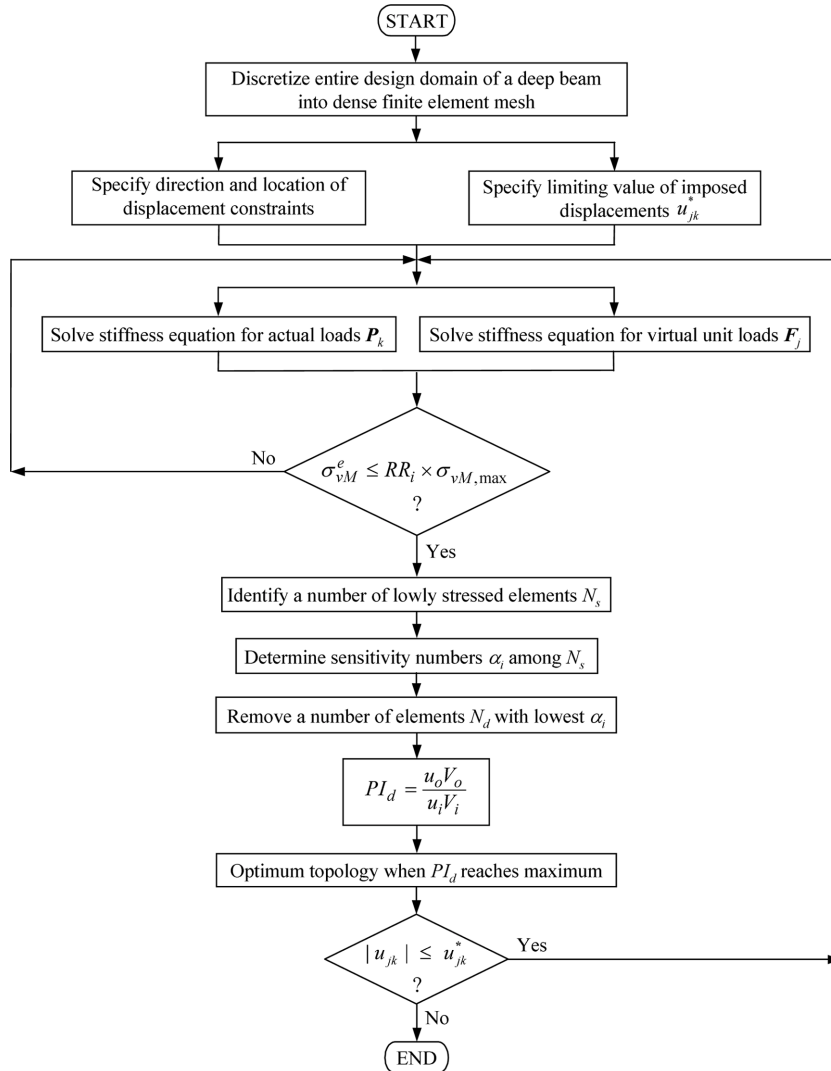


Fig. 1 Flow chart of optimization procedure

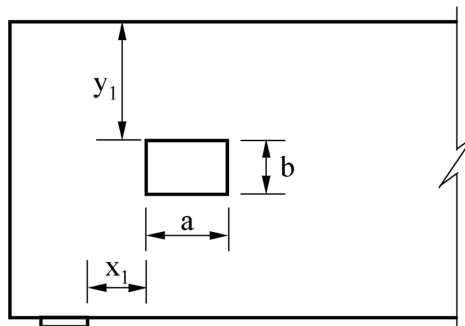


Fig. 2 Illustrative diagram of a deep beam

Table 1 Details of deep beam models

Beam designation	DB1	DB2	DB3	DB4	DB5	DB6	DB7	DB8	DB9	DB10	DB11
Overall dimension (mm × mm)	1950 × 1000	1950 × 1000	1325 × 750	1325 × 750	1060 × 450	1425 × 750	1300 × 750	3000 × 625	3000 × 625	3000 × 625	3000 × 625
Number of opening(s)	1	2	1	2	1	2	2	2	2	2	2
<i>a</i> (mm)	200	200	225	225	200	225	225	125	125	250	250
<i>b</i> (mm)	200	200	150	150	150	150	150	125	125	250	250
<i>x</i> ₁ (mm)	450	150	50	50	0	50	50	875	200	800	125
<i>y</i> ₁ (mm)	400	400	500	500	200	300	500	250	250	200	200
Number of point load(s)	1	1	2	2	1	2	1	2	2	2	2
Magnitude of load(s) (kN)	825	618	97.5	97.5	210	720	97.5	588	902	419	864
Support conditions	S	S	S	S	S	S	S	C	C	C	C
Young's Modulus (×10 ⁴ MPa)	3.145	3.145	3.097	3.097	4.210	2.860	3.097	2.308	2.603	2.583	2.760
Poisson's ratio	0.2	0.2	0.15	0.15	0.2	0.15	0.15	0.2	0.2	0.2	0.2
Thickness of beam (mm)	100	100	100	100	100	100	100	100	100	100	100
Source	D'Arcy 2002	D'Arcy 2002	–	Kong and Sharp 1977	Almeida and Pinto 1999	Foster and Gilbert 1996	–	Ashour and Rishi 2000			

Note: S - simple support; C - continuous support

4. Varying size, location and number of openings

The effect of varying size, location and number of openings on the strut-and-tie model of deep beams is studied through the comparison between four beams, DB1 to DB4, in three groups.

4.1 Group 1: DB1 vs DB2 - square opening(s) at mid-depth of the beams

Group 1 compares DB1 and DB2 of identical dimension and both under single point load and having square opening(s) at mid-depth of the beam. DB1 has a single opening at mid-span whereas DB2 has two openings falling in the compression load transfer paths. The comparisons are shown in Fig. 4. As can be seen in DB1, when the opening is located away from the load path, the compression transfer takes the shortest path between the load and support points, as indicated in Fig. 4(e1). When the opening falls in the compression transfer path, on the other hand, the strut-and-tie model revolutionizes, as indicated in DB2, where the path are re-routed around the opening,

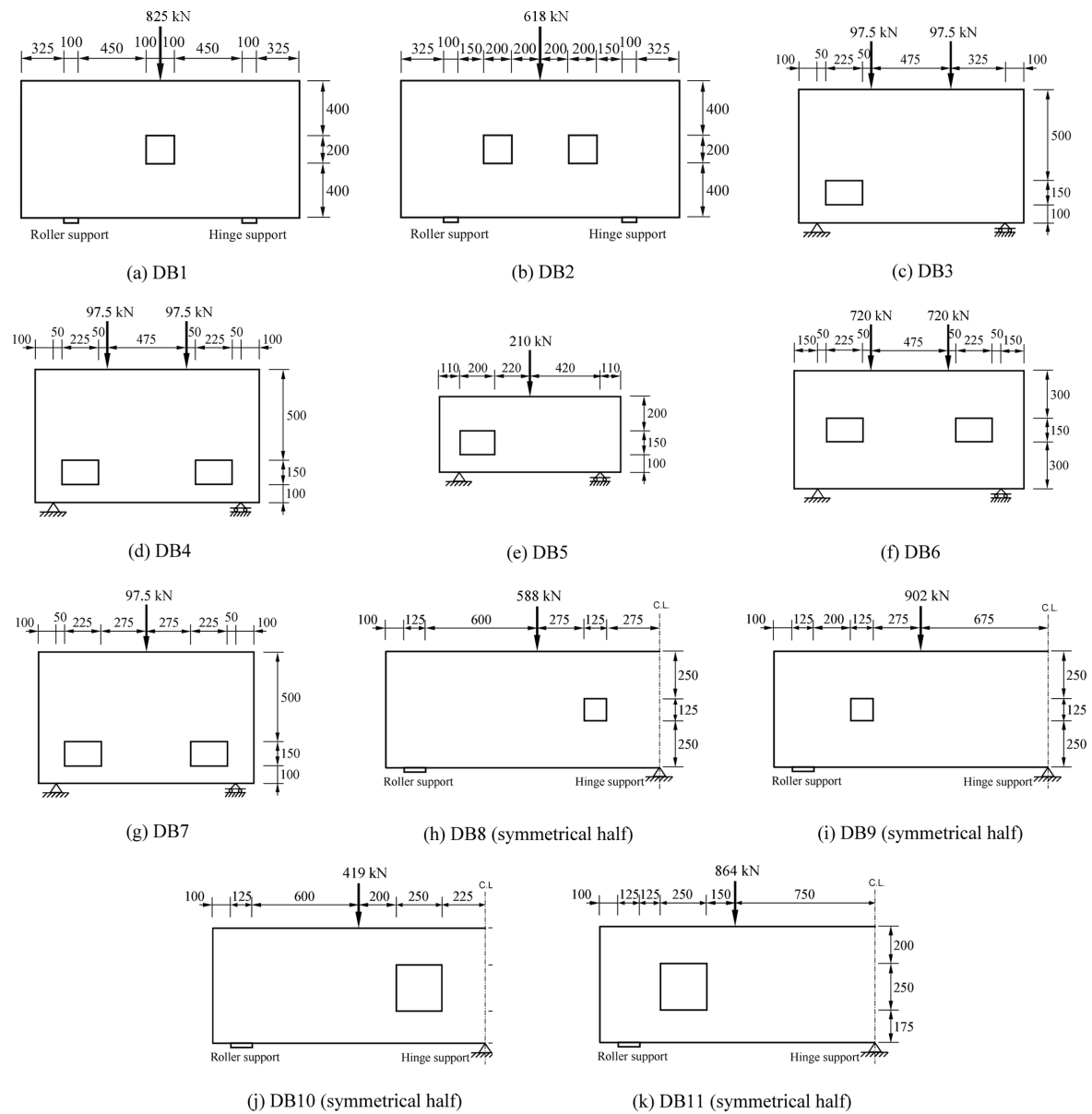


Fig. 3 Configurations of deep beam models

thus introducing tension ties around the opening (see Fig. 4(e2)). As logic would tend to suggest that the compression struts pass the opening on the left- and right-hand sides, while the tension ties connect the compression zones above and below the openings (Parsons and Guan 2003).

4.2 Group 2: DB3 vs DB4 - rectangular opening(s) close to the bottom of the beams

Also of the same dimensions and under two point loads, both DB3 and DB4 have rectangle web

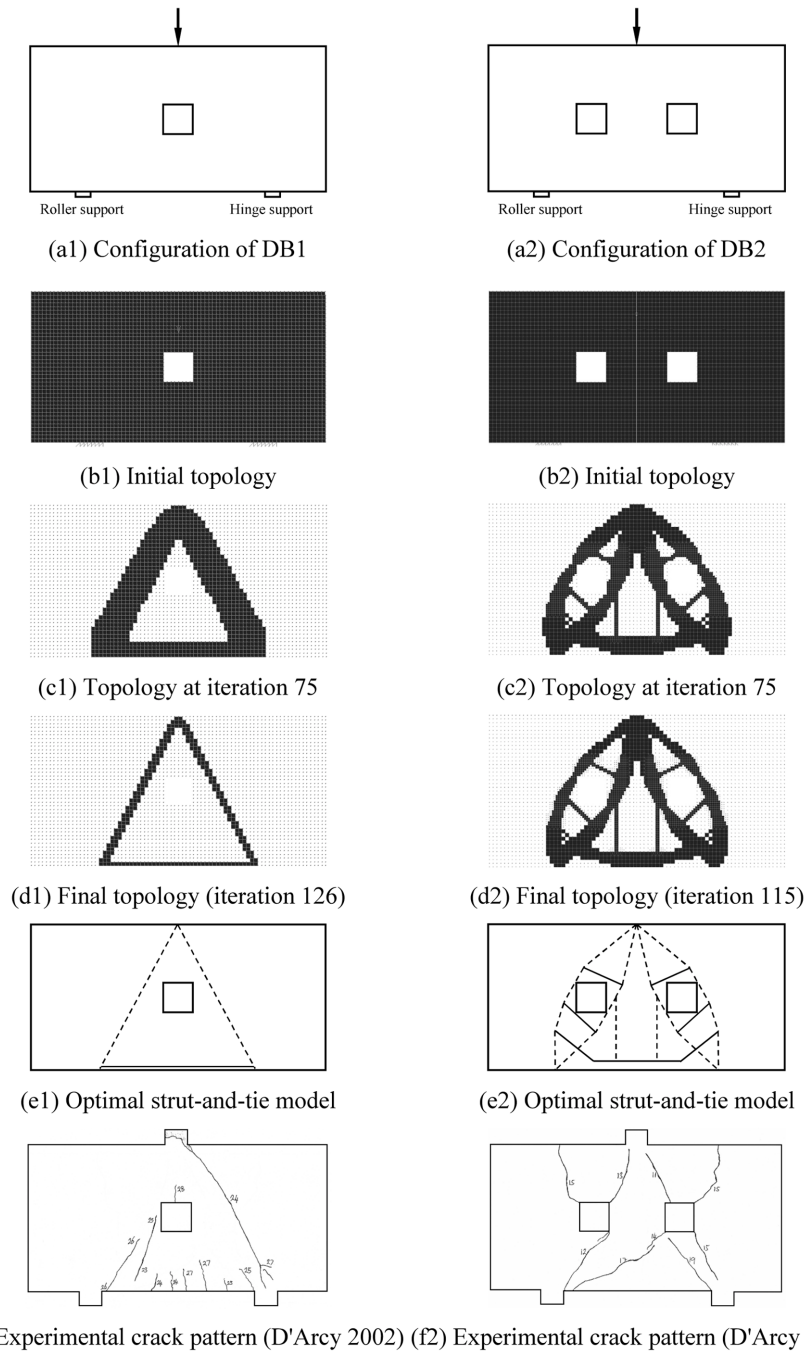


Fig. 4 Comparisons of strut-and-tie models between DB1 and DB2

opening(s) close to the bottom of the beams, as shown in Figs. 5(a1) and 5(a2). In both beams, the opening falls in the compression transfer path. If only one opening is present as in DB3, the strut-and-tie model on the side without an opening becomes relatively simple, as the compression transfer

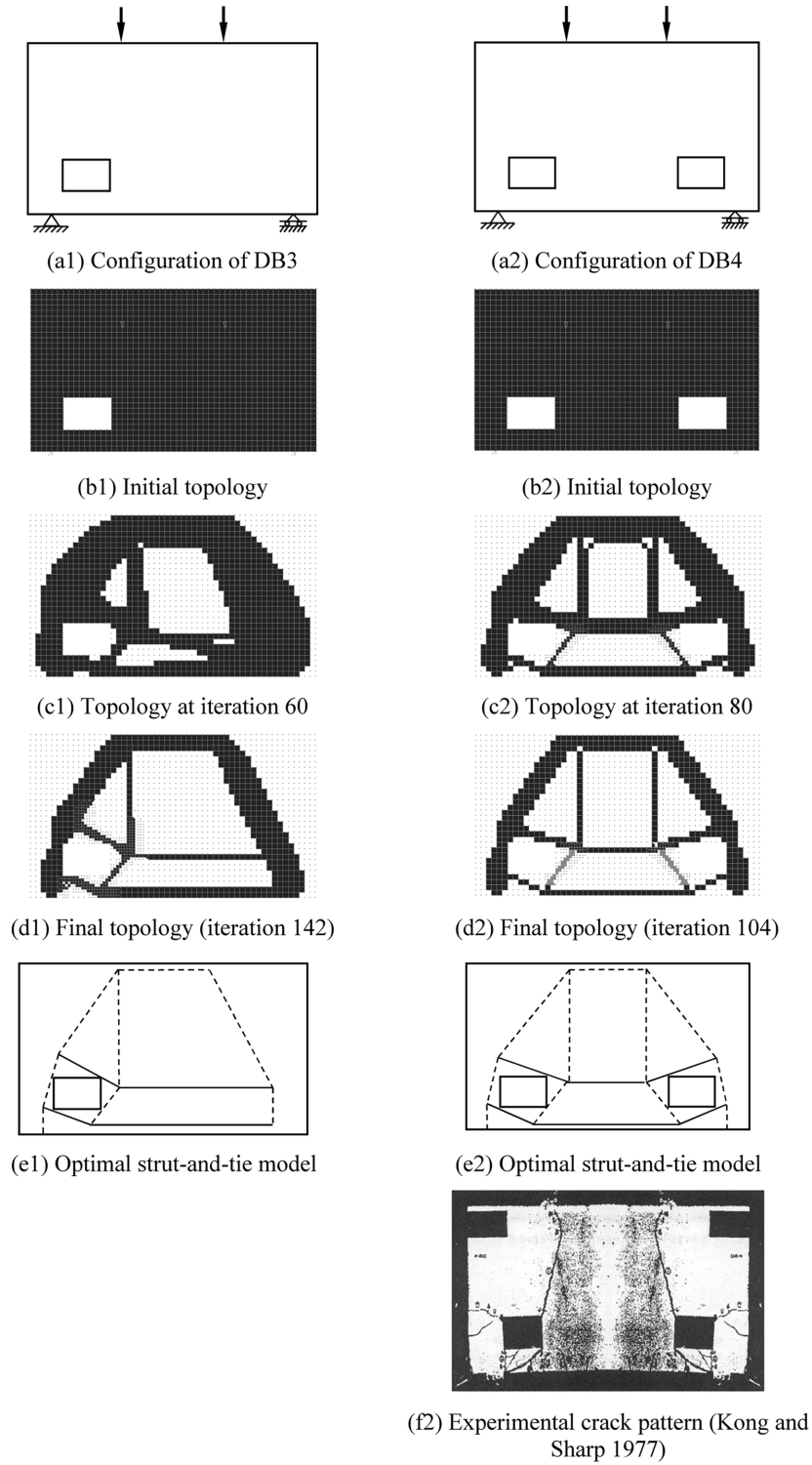


Fig. 5 Comparisons of strut-and-tie models between DB3 and DB4

path runs directly from the loaded area to the support (see Fig. 5(e1)). If two openings are present the strut-and-tie model becomes more complicated on both sides. However as expected, DB4 is symmetrical, hence the strut-and-tie model is consistent on both sides (see Fig. 5(e2)). This factor allows the designer to model only half the beam, saving on computational time.

4.3 Group 3: DB1 vs DB3 and DB2 vs DB4 - location of opening(s)

Comparing DB1 and DB3 (Figs. 4(e1) and 5(e1)) as well as DB2 and DB4 (see Figs. 4(e2) and 5(e2)), the differences in the strut-and-tie model are demonstrated when the position of the openings is moved from the mid-depth to the bottom of the beam. When the opening(s) is lower in the beam there tends to be an addition of two horizontal tension ties that unite both left and right compression transfer, above and below the openings. This is evident in DB3 and DB4.

4.4 Optimal strut-and-tie model vs experimental crack pattern

It should be noted in Figs. 4(f1), 4(f2) and 5(f2) that there are similarities between the experimental observations and the computer generated results. It is generally accepted that the first cracks in deep beams appear at the top and bottom of the openings provided that the opening is in the compression transfer zone. As the load increases these cracks propagate from the top of the opening(s) towards the loaded area(s) and from the bottom of the opening(s) towards the closest support. In addition to this diagonal or shear cracking, flexural cracking can occur at the bottom of the beams. However in relation to the distance that these flexural cracks extend, and the crack width at failure, they are generally considered to be minor issues, and more predominate cracks that occur are shear related. Therefore it is safe to assume that the top and bottom of the opening are under high-tension stresses because that is where the first major cracks appear. It should also be noted that the bottom of the beam also experiences reasonably high-tension forces. Therefore it is logical to place steel reinforcement in these sections to counteract the low-tension capacity of concrete. As the strut-and-tie model is used to determine reinforcement layout it would be expected that tension ties would form in these places. As can be seen in DB1, DB2 and DB4, this is generally what happens. Thus it can be concluded that the computer generated strut-and-tie model does accurately predict where the steel reinforcement is to be placed.

In addition to these counter tension reinforcements other reinforcement may be required. Sometimes in deep beams reinforcement is provided around the opening to counteract cracking at regions of stress concentrations which would occur at the corners of the openings.

5. Varying loading conditions

The effect one or two point loads has on the strut-and-tie model of deep beams with web openings is investigated. In all, six deep beams DB5, 3, 2, 6, 7 and 4 are compared in three groups, viz Groups 4, 5 and 6. Each group has two beams, one is subjected to a mid-span concentrated load and the other under two point loads. The optimization of DB5, 6 and 7 are presented in Figs. 6, 7 and 8 respectively for the three groups. For DB3, 2 and 4 which has been analyzed in Section 4, only their configurations and the corresponding optimal strut-and-tie models are included for comparison.

5.1 Group 4: DB5 vs DB3 - single opening near bottom left corner of the beams

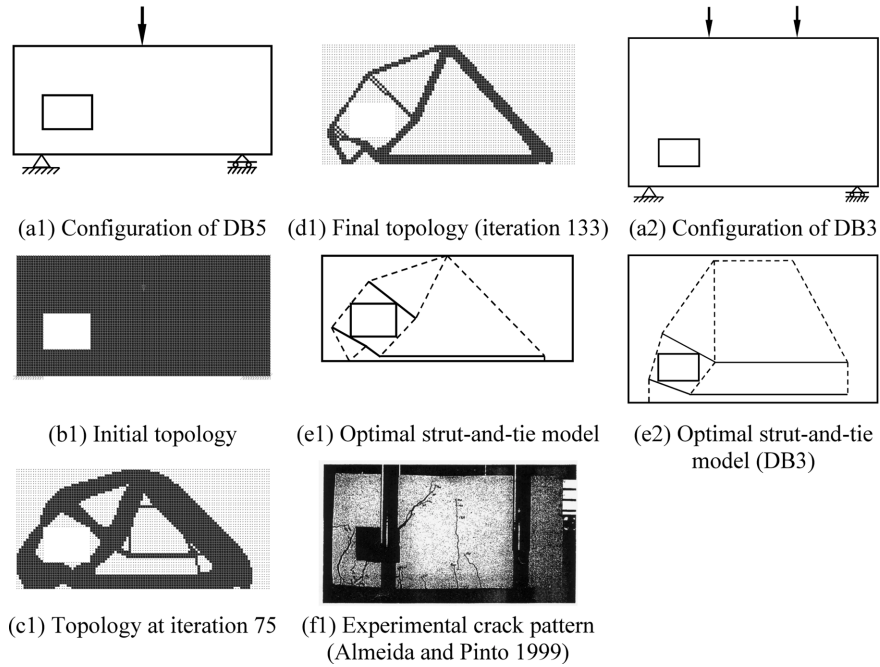


Fig. 6 Comparisons of strut-and-tie models between DB5 and DB3

5.2 Group 5: DB2 vs DB6 - two openings at mid-depth of the beams

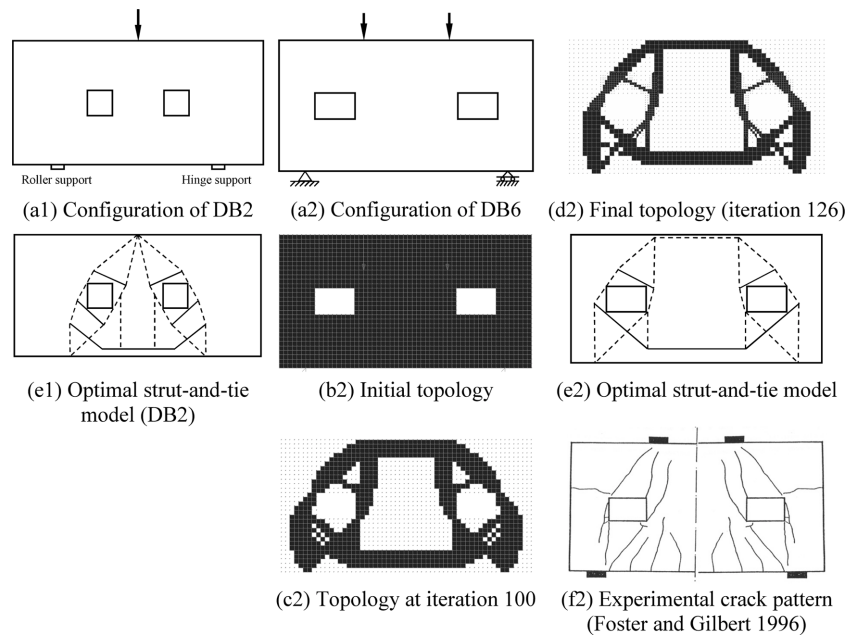


Fig. 7 Comparisons of strut-and-tie models between DB2 and DB6

5.3 Group 6: DB7 vs DB4 - two openings at the bottom of the beams

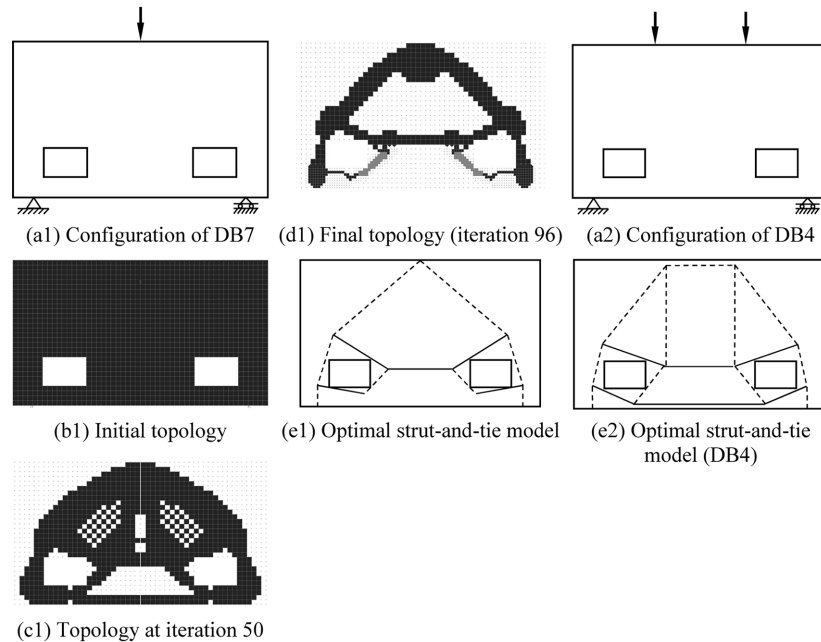


Fig. 8 Comparisons of strut-and-tie models between DB7 and DB4

Similar to the observations discussed in Section 4, if the opening is located away from the load path, the compression transfer takes the shortest route, as apparent in DB5 and DB3. When the opening falls in the compression transfer path, as in all the six beams DB5, 3, 2, 6, 7 and 4, the compression strut is re-routed around the opening, thus introducing tension ties connecting the compression zones above and below the openings. When the experimental crack patterns are available, the resulting optimal strut-and-tie models also agree well with the experimental observations, as compared between Figs. 6(e1) and 6(f1) as well as Figs. 7(e2) and 7(f2).

It is important to note about the loading condition is that when a single concentrated load is present, a triangle-based strut-and-tie model forms, as evident in DB5, DB2 and DB7 (see Figs. 6(e1), 7(e1) and 8(e1)). In this case the left-hand side of the triangle is the left re-routed compression transfer, while the right-hand side is the right compression transfer, with the lower tension tie forming the bottom of the triangle. On the other hand, if two point loads are present a trapezoid-based strut-and-tie model forms, as obvious in DB3, DB6 and DB4 (see Figs. 6(e2), 7(e2) and 8(e2)). The left and right re-routed compression transfers and the bottom of the trapezoid are formed in the same manner as the triangle-based strut-and-tie model, however it is necessary to have an additional horizontal strut between the loaded points to form the top side of the trapezoid.

6. Varying support conditions

The influence on the strut-and-tie model in relation to different support conditions of deep beams is also examined. In all, five deep beams (i.e., DB6, 8, 9, 10 and 11) are optimized and compared in

three groups viz Groups 7, 8 and 9. All the beams are subjected to two concentrated loads. Group 7 compares the difference between a simply supported beam and a continuous beam, both with two web openings. Group 8 deals with two continuous deep beams both with two web openings that are of the same size but different locations. Group 9 is similar to Group 8 in that the locations of openings differ however the size of openings are identical in both beams. The effect different sizes of openings have on the strut-and-tie model is also examined through the comparison between Groups 8 and 9.

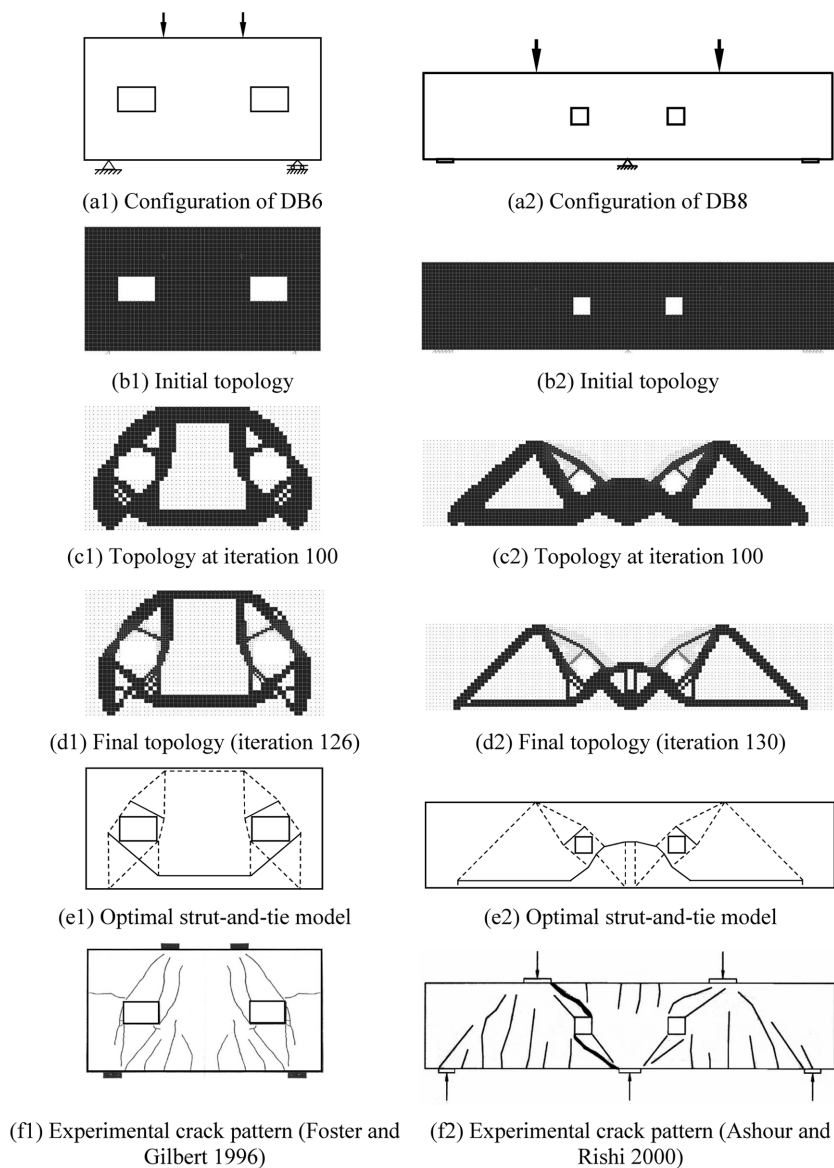


Fig. 9 Comparisons of strut-and-tie models between DB6 and DB8

6.1 Group 7: DB6 vs DB8 - simply supported and continuous beams

A comparison between DB6, a simply supported beam and DB8, a continuous beam is presented in Fig. 9. Note that the optimization outcome of DB6 is reproduced herein for better comparison. Generally in both cases the struts and ties around the openings are similar. This can be seen in both Figs. 9(e1) and 9(e2). The most notable difference however between the two strut-and-tie models, is seen around the internal support of the continuous beam DB8. Over the continuous support an additional horizontal tension tie forms between the compression struts at this particular point. Also, generally two compressive struts form directly over the continuous support and rise vertically up to the newly formed tension tie. This makes the design of a continuous deep beam more complicated than a simply supported counterpart. The experimental crack patterns are also included for comparison (see Figs. 9(f1) and 9(f2)), which confirms the accuracy of the strut-and-tie models.

6.2 Group 8: DB8 vs DB9 - continuous beams with varying locations of small openings

In comparing DB8 and DB9 where the locations of web openings differ (see Fig. 10), it can be noted that there is a major difference between the two strut-and-tie models in the shear spans where there is no web openings. When the opening is located within the interior shear spans (as in DB8), compression struts form in the exterior shear spans following the shortest load path, as indicated in Fig. 10(e1). On the other hand, when the opening is located within the exterior shear spans (as in DB9), the compression struts in the interior shear spans are interrupted by the additional tension ties above the central support, as depicted in Fig. 10(e2). This is not unlike the experimental observation (Ashour and Rishi 2000) where two distinct modes of failure, affected mainly by the location of the openings, were noticed. When the openings are within the interior shear spans like in DB8, the diagonal cracks that formed at the corners of the openings extended both ways towards the load point and support, as highlighted in Fig. 10(f1). For the beam having openings within the exterior shear spans like in DB9, in addition to the diagonal cracks propagating from the opening corners towards the load point and support, another major diagonal crack occurred between the load point and support, which is also highlighted in Fig. 10(f2).

Also included in the comparison are the PI_d curve resulted from Eq. (9) and the volume reduction curve. For beam DB8, Fig. 10(g1) shows that the PI_d value increases from one (1) indicating that the topology of the deep beam is improved by systematically removing inefficient material from the original over-designed area. In addition, the PI_d value reaches the maximum at iteration 130 when the final topology is generated. While the performance index increases, the volume ratio (V/V_o) decreases, as shown in Fig. 10(h1). Similar optimization history is found for beam DB9, as evident in Figs. 10(g2) and 10(h2).

6.3 Group 9: DB10 vs DB11 - continuous beams with varying locations of large openings

Fig. 11 compares the two beams DB10 and DB11, again with different locations of web openings. As compared to those in Group 8, the sizes of the openings are doubled in both beams, however similar outcome is observed.

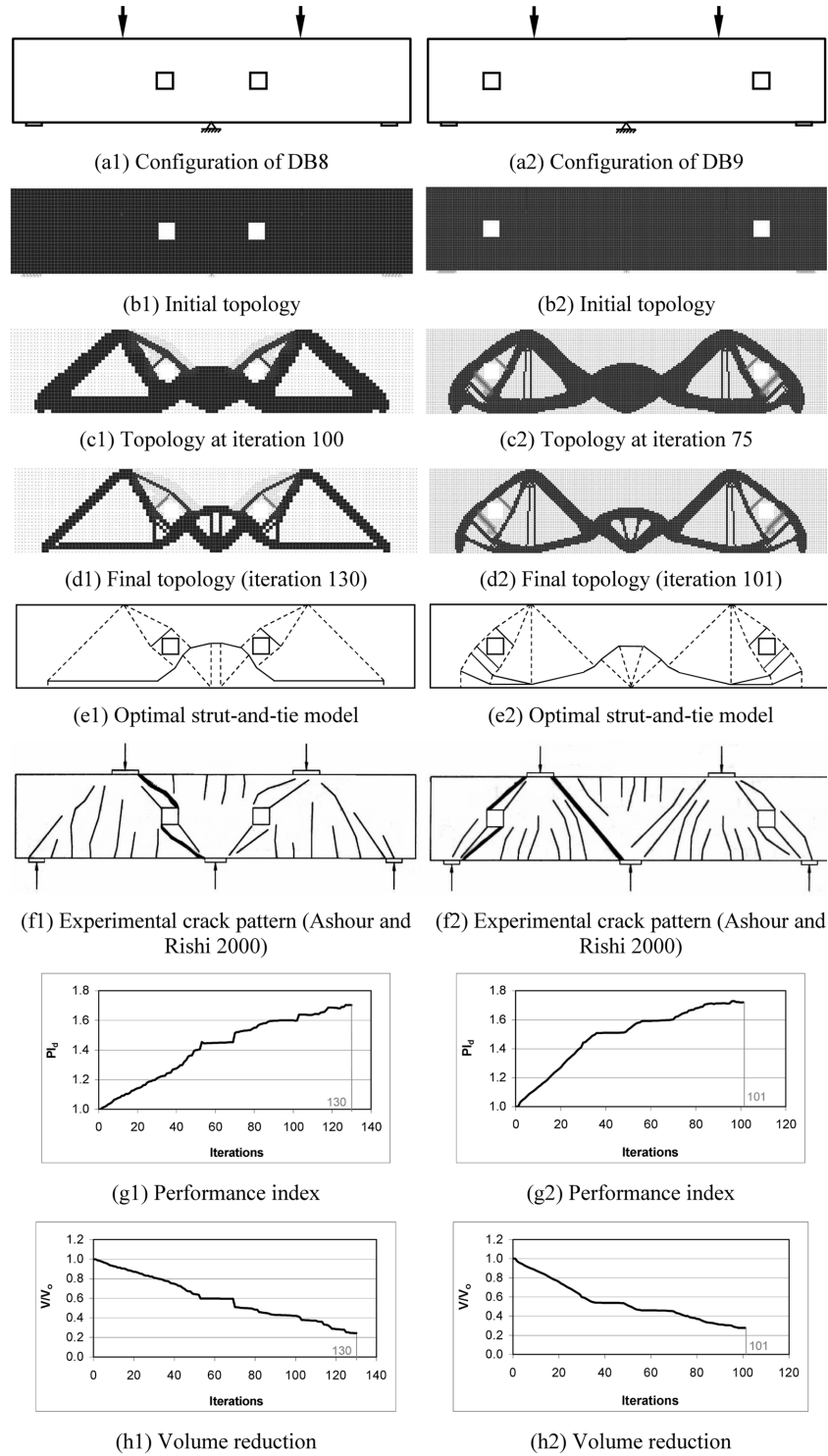


Fig. 10 Comparisons of strut-and-tie models between DB8 and DB9

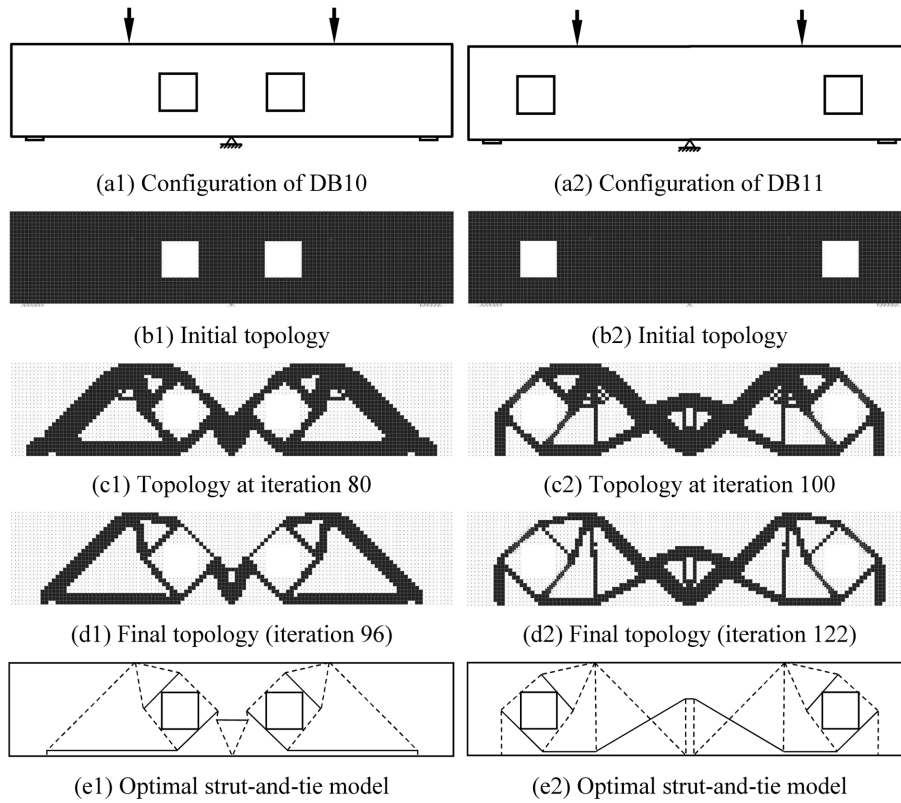


Fig. 11 Comparisons of strut-and-tie models between DB10 and DB11

6.4 Comparison between Groups 8 and 9

For the purpose of comparison, the optimal strut-and-tie models for DB8 to DB11 are reproduced in Fig. 12. As the strut-and-tie models suggest, the modes of failure depend on the locations of web openings, regardless of their sizes. However it is obvious that the larger the opening, the flatter the diagonal cracks joining the corner of the opening and the load point/support. Also from the structural point of view, both the size and location of openings have significant influence on the capacity and serviceability of deep beams.

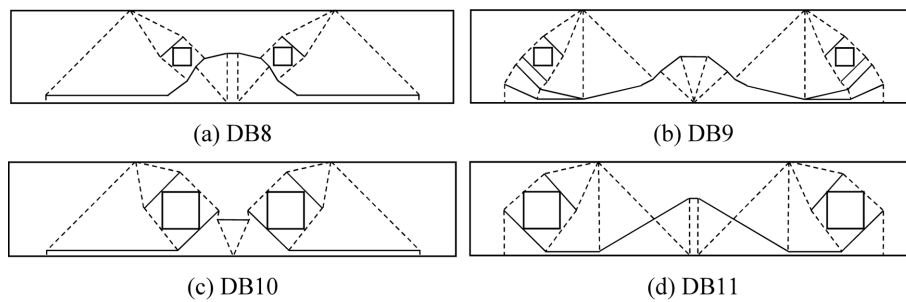


Fig. 12 Comparisons of strut-and-tie models of DB8, 9, 10 and 11

7. Conclusions

In this study, topology optimization of eleven deep beams with web openings is performed under both stress and displacement constraints, by which the system performance (i.e., overall stiffness) of the structure is satisfied. The final topologies, selected based on the maximized performance index, are interpreted into optimal strut-and-tie models. The eleven deep beams are optimized and compared in nine groups, through which the influences on the strut-and-tie model in relation to different size, location and number of openings, as well as different loading and support conditions are examined. The optimal strut-and-tie models achieved are also compared with published experimental crack patterns.

Based on the comparisons made in nine groups, the follow findings are also observed.

(1) In relation to different size, location and number of openings:

If the location of the opening is in the compression transfer zone, the load transfer path is re-routed around the sides of the opening, thus causing the formation of additional tension ties at the top and bottom of the opening. The presence of more than one opening complicates the strut-and-tie model. Further, when the opening(s) are lower in the beams there tends to be an addition of a single horizontal tension tie that unites both left and right compression transfer, above the opening(s).

(2) In relation to different loading conditions:

Under a single point load, a triangle-based strut-and-tie model forms, whereas under two point loads, the strut-and-tie model becomes trapezoid in shape with an additional horizontal strut forming the top side of the trapezoid.

(3) In relation to different support conditions:

In comparing the strut-and-tie models of a simply supported beam and a continuous beam, it has been found that the prominent difference is at around the internal support of the continuous beam, where an additional horizontal tension tie forms between the compression struts. Also, generally two compressive struts form directly over the continuous support and rise vertically up to the newly formed tension tie. This makes the design of a continuous deep beam more complicated than a simply supported counterpart. In addition, numerical results have confirmed the experimental observations in that the modes of failure in continuous deep beams depend on the location of web openings regardless of their sizes.

In summary, the optimal strut-and-tie models generated compared favourably with experimental crack patterns, thereby suggesting the accuracy of the optimal strut-and-tie models in a variety of different situations. The study has provided some insights into various parameters that affect the load transfer mechanisms of concrete deep beams with openings under ultimate load. This in turn would assist detailed reinforcing design of such elements that exhibit complicated structural behaviour.

Acknowledgements

The assistance of a former undergraduate student Mr. Joseph Parsons in carrying out the numerical study at the School of Engineering, Griffith University Gold Coast Campus is gratefully acknowledged.

References

- Almeida, A. and Pinto, N. (1999), "High strength concrete deep beams with web openings", *ACI Special publications*, **SP-1**(186), 567-613.
- American Concrete Institute (ACI) (2002), *Building Code Requirements for Structural Concrete (ACI 318-02) and Commentary - ACI318R-02*, Detroit, Michigan.
- Ashour, A. and Rishi, G. (2000), "Tests of reinforced concrete continuous deep beams with web openings", *ACI Struct. J.*, **97**(3), 418-426.
- Ashour, A.F. (1997), "Tests of reinforced concrete deep beams", *ACI Struct. J.*, **94**(1), 3-12.
- British Standards Institution (BSI) (1997), *BS8110: 1997, Parts I and II, Structural Use of Concrete*, London.
- D'Arcy, M. (2002), "The behaviour of simply supported concrete deep beams with high strength concrete", BEng Thesis, School of Engineering, Griffith University Gold Coast Campus, Australia.
- European Committee for Standardisation (1992), *Eurocode 2, Design of Concrete Structures, Part I: General Rules and Rules for Buildings*, ENV 1992-1-1, Brussels.
- Foster, S. and Gilbert, R. (1996), *Tests on High Strength Concrete Beams*, UNICIV Report, R-354.
- Foster, S. and Gilbert, R. (1998), "Experimental studies on high strength concrete deep beams", *ACI Struct. J.*, **95**(4), 382-390.
- Guan, H., Chen, Y.J. and Loo, Y.C. (2001), "Topology optimisation of bridge type structures with stress and displacement constraints", *Int. J. Computational Engrg. Sci.*, **2**(2), 199-221.
- Kong, F.K. (1990), *Reinforced Concrete Deep Beams*, Blackie and Sons Ltd, Glasgow.
- Kong, F.K. and Sharp, G.R. (1977), "Structural idealization for deep beams with web openings", *Magazine of Concrete Res.*, **29**(99), 81-91.
- Liang, Q.Q., Xie, Y.M. and Steven, G.P. (2000), "Topology optimisation of strut and tie model in reinforced concrete structures using an evolutionary procedure", *ACI Struct. J.*, **97**(2), 322-330.
- Mansur, M.A. and Alwis, W.A.M. (1984), "Reinforced fibre concrete deep beams with web openings", *Int. J. Cement Composites and Lightweight Concrete*, **6**(4), 263-271.
- Maxwell, B. and Breen, J. (2000), "Experimental evaluation of strut and tie model applied to deep beam with opening", *ACI Struct. J.*, **97**(1), 142-148.
- Parsons, J. and Guan, H. (2003), "Optimisation of strut-and-tie model in deep beams with openings", *Proc. EURO-C Conf. 2003*, St. Johann Im Pongau, Austria, March.
- Rogowsky, D.M., MacGregor, J.G. and Ong, S.Y. (1986), "Test of reinforced concrete deep beams", *ACI Struct. J.*, **83**(4), 614-623.
- Standards Association of Australia (SAA) (2002), *AS3600-2002: Concrete Structures*, Sydney, Australia.
- Tan, K.H., Kong, F.K. and Weng, L.W. (1997a), "High strength concrete deep beams subject to combined top-and bottom-loading", *The Struct. Engineer*, **75**(11), 191-197.
- Tan, K.H., Kong, F.K., Teng, S. and Guan, L. (1995), "High-strength concrete deep beams with effective span and shear span variations", *ACI Struct. J.*, **92**(S37), 395-405.
- Tan, K.H., Kong, F.K., Teng, S. and Weng, L.W. (1997b), "Effect of web reinforcement on high strength concrete deep beams", *ACI Struct. J.*, **94**(5), 572-582.
- Tan, K.H., Tang, C.Y. and Tong, K. (2003a), "A direct method for deep beams with web reinforcement", *Magazine Concrete Res.*, **55**(1), 53-63.
- Tan, K.H., Teng, S., Kong, F.K. and Lu, H.Y. (1997c), "Main tension steel in high strength concrete deep and short beams", *ACI Struct. J.*, **94**(6), 752-768.
- Tan, K.H., Tong, K. and Tang, C.Y. (2003b), "Consistent strut-and-tie modelling of deep beams with web openings", *Magazine Concrete Res.*, **55**(1), 65-75.
- Xie, Y.M. and Steven, G.P. (1997), *Evolutionary Structural Optimisation*, Springer-Verlag, London.